226

Design of a Long-Range Single-Mode OTDR

MARTIN P. GOLD

Abstract—**The design of a high-performance single-mode optical time-domain reflectometer (OTDR) is discussed. The approach uses a low-noise receiver with a p-i-n diode detector and transimpedance amplifier together with multichannel digital averaging. A dynamic range of 30 dB one way at 1.3 μm is demonstrated with a laser diode source, and with a Nd:YAG laser source the dynamic range is 41 dB one way.**

I. Introduction

OPTICAL TIME-DOMAIN reflectometry [1]-[3] is now well established for characterizing loss and imperfections in multimode optical fibers. The technique involves launching a short pulse of light into the fiber and measuring the temporal behavior of the backscattered light which returns to the launch end. For long-distance optical communications, the emphasis is now shifting to single-mode fibers operating at longer wavelengths, owing to the greater bandwidths and larger distances between repeaters which can be achieved. However, the optical time-domain reflectometry (OTDR) technique is more difficult in single-mode fibers, and although a considerable effort [4]-[15] has been made recently to develop single-mode OTDR measurements, most of the approaches tried have drawbacks for practical application. The requirements for an OTDR for long-distance single-mode fiber systems are considered in the next section, and the extent to which the available approaches fulfill these requirements is examined.

II. Requirements for a Long-Range OTDR

Range: For measurements on fiber cables during and after installation, the reflectometer must be able to detect the backscatter signal to at least half the maximum distance between repeaters. However, it is much more useful if the measurement can cover the entire fiber span between repeaters as it is then possible to check the integrity of the complete fiber length from one end, and if required, the precise loss of the fiber, splices, and other features can be determined by repeating the measurement from the other end of the fiber, and then averaging the two results [16], [17]. Alternatively, with sufficient measurement dynamic range, the folded-path OTDR technique [18] can be used to obtain the information available from both ends of the fiber by means of a single measurement employing a reflector at the far end of the fiber. The maximum fiber attenuation envisaged between repeaters at present for long-wavelength systems operating at bit rates of $\gtrsim$ 100 Mbit/s is about 30 dB.

Manuscript received June 4, 1984. This work was supported by the UK Science and Engineering Research Council and by Pirelli General.

The author is with the Department of Electronics, The University, Southampton, SO9 5NH England.

Portability: Whereas for laboratory and factory measurements the portability of OTDR equipment is of little significance, the most critical application for dynamic-range performance is in the measurement of fiber cables during and after installation, where a compact and light apparatus is greatly advantageous.

Resolution: There is a trade-off between the dynamic range and the spatial resolution which can be obtained on the backscatter trace, and so for optimum range with long-distance measurements the minimum useful resolution should be adopted. This resolution corresponds to the ability to determine reliably the fiber section in which a fault occurs. The faulty section could then either be replaced in entirety, or a further, short-range measurement with higher resolution could be performed. Since the fiber sections are typically of the order of 1 km in length, a resolution of 100 m should be sufficient for long-range measurements. The resolution l, is related to the probe-pulsewidth τ by

$$l = \tfrac{1}{2} v_g \tau \tag{1}$$

where v_g is the group velocity in the fiber. Thus a resolution of 100 m corresponds to a pulsewidth of 1 μs, and the optical receiver bandwidth must be sufficient that the detected probe-pulse is not significantly broadened from this value.

Measurement Wavelength: The guidance properties of single-mode fibers are strongly wavelength dependent and it is therefore important that the OTDR measurement should match the intended operating wavelength of the optical fiber. It is often suggested that backscatter measurements made at a different wavelength can be interpreted by appropriate scaling of the attenuation the operating wavelength, but the presence of any bends or other features in the fiber is likely to lead to erroneous results. This could be severely misleading in fault-finding applications where such a feature might cause a significant loss at the operating wavelength, but not at the measurement wavelength, or vice versa.

Polarization Insensitivity: The probe-pulse from a single-mode laser is normally polarized, and the Rayleigh scattering process preserves the state-of-polarization of the probe-pulse at the scatter point (apart from a small degree of depolarization due to material anisotropy [19], [26]). The backscatter signal from single-mode fiber will therefore be polarized, and with standard telecommunications (i.e., not polarization-maintaining) fibers the state-of-polarization will vary along the backscatter trace owing to intrinsic and extrinsic fiber birefringence. While this polarization information may be used to investigate the polarization properties of the fiber [20]-[23], the changing polarization of the scatter return

0733-8724/85/0200-0039$0.100

will also cause amplitude modulations of the backscatter signal in conventional OTDR measurements if the efficiency of the receiving optics or of the detection process is polarization dependent. Such amplitude modulations mask the local attenuation information in the backscatter signal and, therefore, reduce the usefulness of the OTDR technique. The problem can be alleviated to some extent by mechanically manipulating the fiber to scramble the state-of-polarization, but the most effective solution is to avoid any polarization sensitivity in the return path of the OTDR apparatus.

In addition to the above criteria, a practical OTDR system must have the ability to cope with reflections from non-index-matched joints and breaks in the fiber. Thus the optical receiver must have a large dynamic range and a rapid recovery from overload. Alternatively, an optical gating arrangement can be employed.

It can be seen from the above requirements that most of the long-range single-mode OTDR systems reported to date are not ideal for practical OTDR measurements. For example, although the Raman OTDR approach [11] achieves the necessary dynamic range, it is not viable for portable apparatus as both a high power Nd:YAG laser, and liquid nitrogen cooling for the detector are used. In addition, the Raman process converts the probe-pulse to longer wavelengths so that the measurement wavelength varies with distance along the fiber, and it is consequently difficult to interpret attenuation information.

If the requirements of dynamic range and portability are taken together, then only the heterodyne detection [13] and low-noise direct detection [12], [15] approaches appear suitable. However, the former requires a laser source with a narrow linewidth, and at present suitable portable sources are not readily available for the normal 1.3-μm single-mode fiber operating wavelength. Also, the use of coherent detection introduces polarization dependence into the detection process, since only the polarization component of the backscattered light which matches the local oscillator state-of-polarization is detected. In practice the advantage in sensitivity available from coherent detection over direct detection is offset by the higher probe-pulse powers obtainable from the lasers of greater spectral width which can be employed with direct detection.

The low-noise direction detection approach is adopted in the present contribution which will analyze the design of a high-performance long-range OTDR system which can fulfill all of the above-mentioned requirements for a practical apparatus.

III. Range Calculation

The most important performance parameter for a long-range OTDR is the maximum range at which faults in the fiber can be located. In practice, this range is defined in different ways depending on the type of fault being considered. For example, a conservative figure is given by the range to which fiber attenuation can be measured to a specified accuracy (e.g., 0.1 dB), and a rather larger figure is given by that at which a 4-percent reflection can be located. The latter is certainly optimistic as a break in the fiber is unlikely to result in a perfect cleave with a perpendicular end face. A straightforward, but realistic criterion for fault location which will be adopted here is *the range at which the signal from Rayleigh scattering becomes equal to the rms noise.* The range is most conveniently expressed in terms of the maximum fiber attenuation which can be penetrated or in "dB one way."

Using the above definition, the dynamic range R is given by the ratio of the Rayleigh scattering signal received from the near end of the fiber to the optical sensitivity of the receiver P_n. The backscatter power P_s received at time t from a uniform fiber is given by

$$P_s(t) = P_0 \tau \eta \exp(-\alpha v_g t) \tag{2}$$

where P_0 is the effective launch power of the probe-pulse, η is the backscatter factor [24] of the fiber, and α is the attenuation constant of the fiber. The effective launch power accounts for the losses in the optics of the OTDR, and is equal to the actual power launched into the fiber multiplied by the transmission efficiency of the return optical path from the fiber to the detector. The dynamic range is then

$$R = \frac{1}{2} \cdot 10 \log_{10} \left(\frac{P_s(0)}{P_n} \right) = 5 \log_{10} \left(\frac{P_0 \tau \eta}{P_n} \right) \tag{3}$$

where the factor of $\frac{1}{2}$ is inserted to give a one-way range figure. The pulsewidth has previously been given a maximum value of $\tau = 1$ μs. The backscatter factor η depends on the parameters of the fiber under measurement [25], [26], but for a typical single-mode fiber its value is around $\eta = 10$ W/J at a wavelength of 1.3 μm. Inserting these values in (3), and putting $P_0 = 1$ mW, then for a range of 25 dB a receiver sensitivity of $P_n = 100$ fW is required.

The receiver sensitivity is normally enhanced by averaging the backscatter waveform from many pulses, and multichannel digital averaging provides the most efficient averaging technique [27]. It has previously been reported [4] that the maximum signal-to-noise ratio improvement obtained by digital averaging is 50 dB (electrical) or 25 dB (optical), but experiments performed with a commercial digital averager (Tracor Northern TN-1550) suggest that the amount of noise reduction is limited in practice only by the time taken. (Note that in this context the signal averaging is concerned with the recovery of weak signals buried in noise, rather than obtaining signals with an already high signal-to-noise ratio with very high accuracy, where the amount of noise reduction achievable will be limited by the linearity of the A to D converter). The averager has a 10-bit resolution with a 2-μs sample interval, but the data from two successive traces are interleaved to give a 1-μs sample spacing. Fig. 1 shows the amount of noise reduction which was measured as a function of the number of averages up to 8×10^6. The results do not show any significant deviation from the straight line which corresponds to the theoretically expected noise reduction equal to the square root of the number of averages. A measurement time limit of 20 min allows 10^6 traces to be averaged with a 2-kHz repetition rate, providing a 30-dB (optical) noise reduction. Thus in the above example the receiver sensitivity required before averaging becomes 100 pW. In practice, an OTDR receiver with an even greater sensitivity can be achieved by design optimization, which will be discussed in the next section.

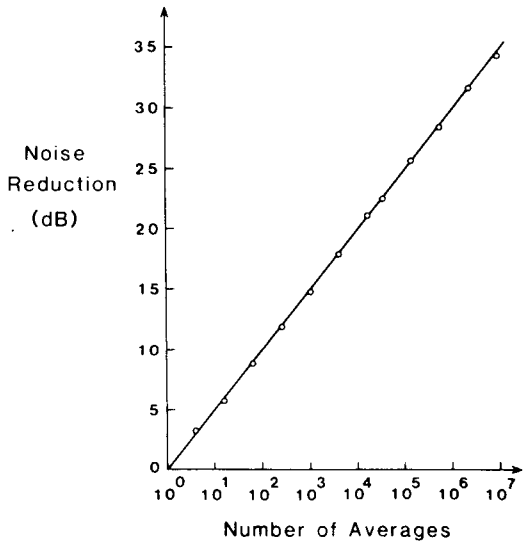

Fig. 1. Noise reduction by digital averaging measured over 200 sample points as a function of the number of averages.

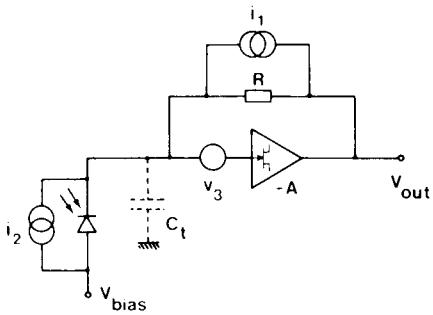

Fig. 2. Chief noise sources in an optical receiver.

IV. Receiver Optimization

The sensitivity of an optical receiver can be limited by various noise sources, both in the detector and in the following amplifier. A low-noise optical receiver can be achieved by using either a high-impedance [28] or a transimpedance [29] preamplifier. The latter type is preferred for amplifying backscatter signals owing to its superior dynamic range, but the noise performance is the same in both cases (the feedback resistor of the transimpedance amplifier becomes the load resistor in the high impedance case). Fig. 2 shows the chief noise sources for a photodiode connected to a transimpedance amplifier. For the bandwidths normally employed for backscatter measurements (i.e., $\lesssim$10 MHz) an amplifier incorporating a silicon JFET at the front end will provide the best noise performance [30]. The equivalent noise generators shown in the diagram are i_1, for the thermal noise of the feedback resistor R, i_2, for the shot noise of the detector dark current I_d, and v_3 for the thermal noise of the FET. The noise spectral densities are given by

$$S_{i_1} = 4kT/R \quad (A^2/\text{Hz}) \tag{4}$$

$$S_{i_2} = 2eI_d \quad (A^2/\text{Hz}) \tag{5}$$

$$S_{v_3} = \frac{2.8kT}{g_m} \quad (V^2/\text{Hz}) \tag{6}$$

where k is Boltzmann's constant, T is the absolute temperature, e is the electronic charge, and g_m is the transconductance of the FET. The FET also has an input noise current consisting of two compcnents: shot noise from the gate leakage current, and frequency-dependent thermal noise induced from the channel through the gate capacitance [31]. Both of these terms can be neglected because the gate leakage current is small (<0.1 nA) compared with the detector dark current, and the effect of the induced gate current is small compared with the effect of v_3. v_3 appears across the total input capacitance C_t, and thus causes an input noise current, i_3 with spectral density

$$S_{i_3} = \frac{2.8kT\omega^2 C_t^2}{g_m} \quad (A^2/\text{Hz}) \tag{7}$$

and, therefore,

$$i_3^2 = \frac{2.8kT(2\pi)^2\, C_t^2 B^3}{3g_m} \quad (A^2) \tag{8}$$

where ω is the angular frequency, and B is the bandwidth. S_{i_3} increases with frequency at a rate of 6 dB/octave, whereas S_{i_1} and S_{i_2} have a white spectrum. The relative contributions of the noise sources can, therefore, only be compared with a known system bandwidth. For long-range ODTR measurements, where a resolution of 100 m is sufficient, the bandwidth required for the receiver is approximately 500 kHz, a figure which will be adopted for the purposes of comparing the noise sources.

The value of i_3 is determined by the ratio C_t^2/g_m. This noise source is therefore minimized by choosing an FET with a low input capacitance and high g_m, and by using a small-area detector to reduce its contribution to the input capacitance. Since the ratio C_{in}/g_m is essentially constant for a given FET material, then neglecting stray capacitances, the minimum value of C_t^2/g_m will be obtained when the capacitance of the detector is equal to the input capacitance, C_{in} of the FET [30]. Inserting typical values, C_t = 8 pF, $g_m = 5 \times 10^{-3}\ \Omega^{-1}$, and B = 500 kHz in equation (8) gives i_3 = 15 pA.

The noise contribution, i_1 from the feedback resistor is reduced by increasing the resistor value, and can be made small compared with i_3 if the resistor is made sufficiently large. However, the bandwidth of the receiver is given by

$$B = \frac{A}{2\pi R C_t} \tag{9}$$

where A is the open-loop voltage gain of the amplifier. Therefore, in order to maintain a given bandwidth, A must be increased in proportion with the feedback resistor value. For the relatively modest bandwidths required for long-range measurements, very large open-loop voltage gains can be achieved with careful circuit design and layout. In our case a feedback resistor value of 500 MΩ has been achieved, which gives a noise contribution, i_1 = 4 pA. The open-loop voltage gain of the amplifier is approximately 20 000 and the closed-loop bandwidth is 850 kHz at - 3 dB (electrical).

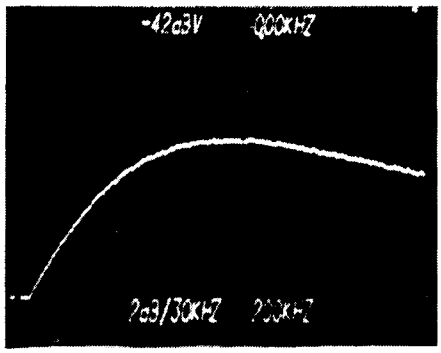

(a)

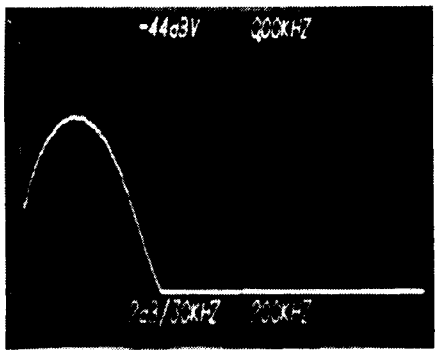

(b)

Fig. 3. Spectral analysis of noise at output of optical receiver (Horizontal scale: 0 to 2 MHz, vertical scale: 2 dB per division). (a) Before low-pass filter. (b) After low-pass filter.

The remaining noise source to be considered arises from the detector dark current. An avalanche photodiode is normally chosen for backscatter receivers, but for the longer wavelengths the only commercially available devices are germanium APD's, which have high dark currents even for small-area devices, and consequently their noise would completely dominate that of the amplifier, even when biased for unity gain. In this application GaInAs or HgCdTe p-i-n diodes provide a superior noise performance. Both types of p-i-n diodes have been used successfully with the low-noise amplifier. The GaInAs device tried (Plessey, type HRD200) had a dark current of 5 nA at room temperature, which would give a noise current, i_2 = 28 pA. In order to reduce the dark current, the device was mounted on a single-stage thermoelectric cooler to give an operating temperature of -18°C, at which point the dark current is reduced to about 0.5 nA, and thus i_3 becomes the dominant noise source. The HgCdTe detector [32] had a lower room-temperature dark current of 0.8 nA, which provides a satisfactory noise performance operated without any cooling. The rapid progress being made in the performance of III-V long wavelength APD's may soon lead to devices which can provide an improvement in detection sensitivity in this application.

Fig. 3(a) shows the noise spectrum of the optical receiver measured on a spectrum analyzer. Above 50 kHz, the noise spectral density rises steadily with frequency as is expected from the dominant noise term i_3 until the closed-loop bandwidth is curtailed by the single pole with time-constant $\tau = RC_t/A$. Beyond this point, the noise density becomes proportional to the open-loop voltage gain $A(\omega f)$, which falls to -3 dB

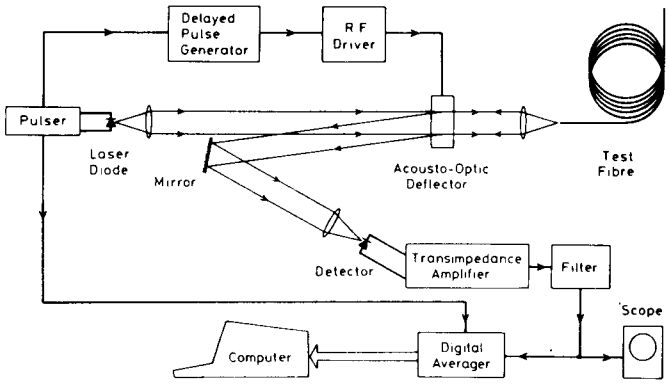

Fig. 4. Schematic diagram of OTDR apparatus.

at about 3 MHz. Thus the noise spectrum at the receiver output is dominated by noise energy above its cutoff frequency, and low-pass filtering of the output signal is clearly required to achieve the equivalent input noise currents calculated above. However, it is essential that any such filter should provide negligible distortion of the signal in the time domain, which limits the initial slope of the filter. A six-pole filter with a Bessel response and a 1-μs rise time was chosen to give maximum attenuation of the high frequency noise while maintaining the 100-m resolution of the OTDR system. Fig. 3(b) shows the noise spectrum of the receiver after passing through the filter. The noise density starts to fall off above 300 kHz, and the total noise output is significantly reduced.

The total equivalent input noise of the receiver in the bandwidth defined by the filter was measured to be 17 pA using the cooled GaInAs photodiode, and 19 pA with the HgCdTe detector at room temperature. The latter device has a slightly higher responsivity so that in both cases the optical sensitivity before averaging is 30 pW.

V. OTDR System

The complete OTDR apparatus is shown schematically in Fig. 4. The light source is a 1.3-μm inverted-rib-waveguide laser diode [33], which is driven to give pulses of 1-μs duration. The laser light is collimated by a high numerical aperture 4-mm focal-length lens system in order to pass through the 2-mm-diam aperture of the acoustooptic deflector (AOD). The light is then focused into the test fiber by an 8-mm focal-length lens. The peak power launched into the fiber is 10 mW.

The AOD provides optical gating [6] for the return path; the backscatter signal arrives at the receiver when the AOD is turned on. Thus the Fresnel reflection from the front end of the fiber can be attenuated, and the backscattered light from the near part of the fiber can be shut off while the far end of the fiber is being measured, which reduces the dynamic range requirements on the optical receiver. A $PbMoO_4$ device was chosen for the AOD as this material has a figure of merit which is virtually independent of the state of polarization of the light [34], and so introduces negligible polarization sensitivity into the path of the backscattered light. The RF drive frequency is 80 MHz, and with a drive power of 1.2 W, the deflection efficiency at 1.3 μm is about 50 percent. The transmission efficiency of the complete return optical path is about 30 percent so that the effective launch power, P_0 = 3 mW. The backscatter signal is detected by the optical re-

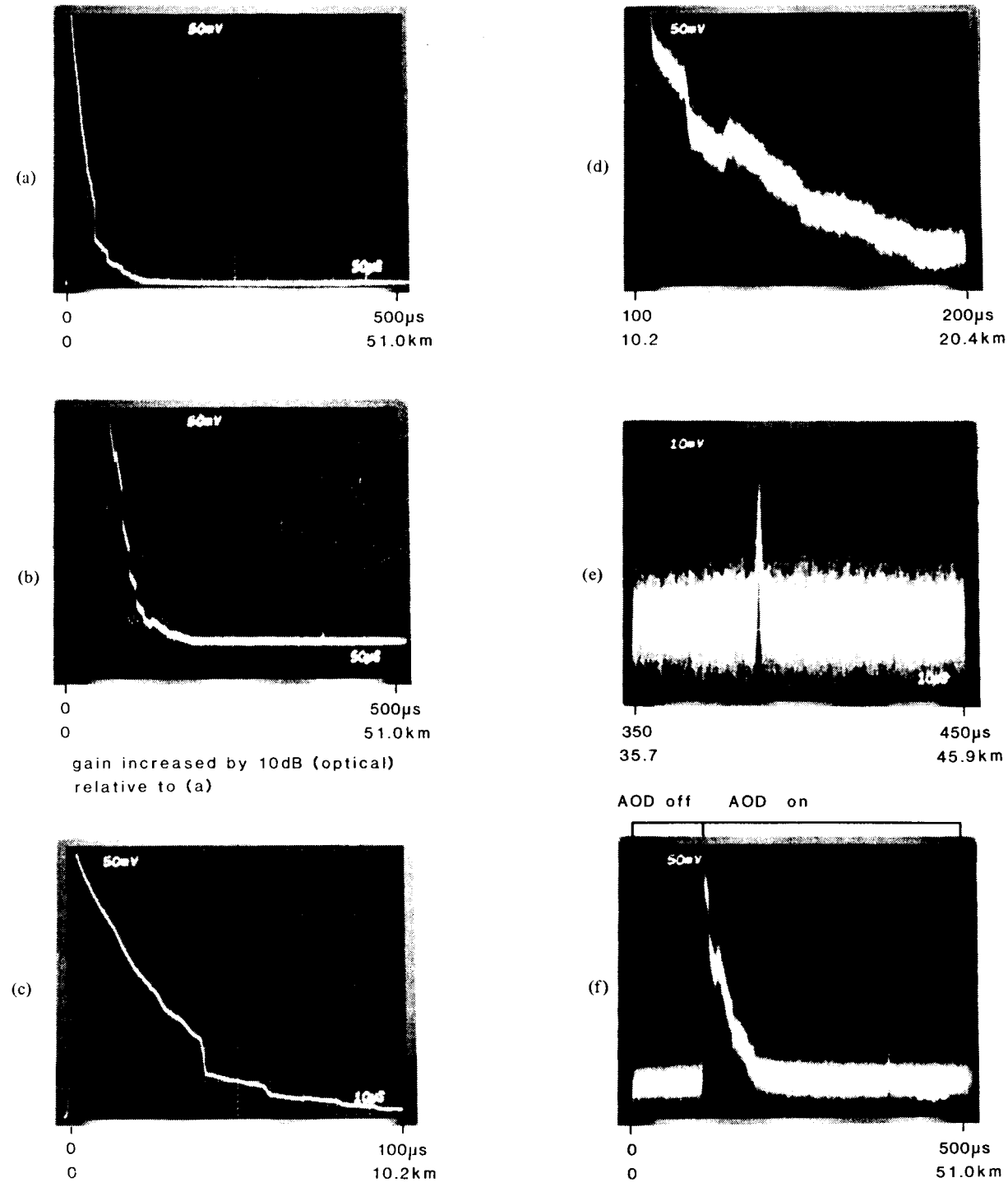

Fig. 5. Real-time backscatter traces obtained from a 39.5-km fiber with a laser diode source.

ceiver described in Section IV, and the signal at the output of the filter can either be viewed in real time on the oscilloscope, or averaged by the digital averager (described in Section III). The data from the averager are transferred to a computer for further averaging and storage.

VI. Experimental Results

With an effective launch power $P_0 = 3$ mW, and a receiver sensitivity $P_n = 30$ pW, then according to (3) a dynamic range of 15 dB should be achieved before any averaging. After 10^6 averages, the range should be increased by 15 dB to give a range of 30 dB. These figures are confirmed by the experimental results which have been obtained with the system described. Measurements were performed on a 39.5-km single-mode fiber length consisting of 22 sections joined by arc-fusion splices. The nominal lengths of the sections are as follows: 1 X 4 km, 1 X 2 km, 11 X 1.1 km, 8 X 2.2 km, and a final 3-km length. The total fiber attenuation is 30 dB at the operating wavelength of 1.3 μm including 7 dB for the loss of the splices.

Fig. 5 shows oscilloscope traces of the unaveraged backscatter signal obtained at the output of the filter. The complete fiber length is shown in (a) and (b), while (c) and (d) show the first 20 km in greater detail. These real-time traces

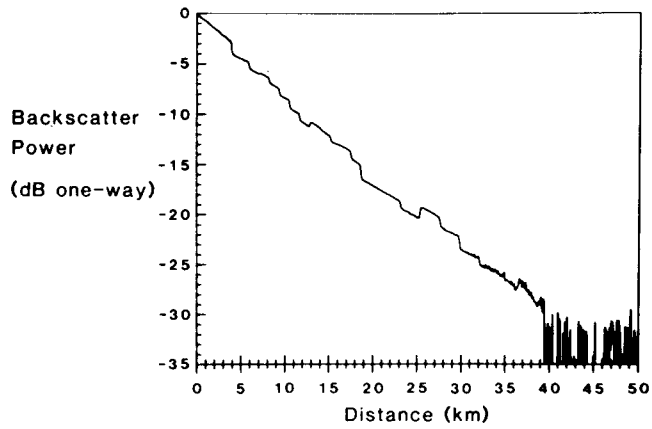

Fig. 6. Logarithmic plot of averaged backscatter trace obtained from a 39.5-km fiber with a laser diode source.

are found to be stable and reproducible, and do not show any polarization modulation or source coherence effects [26]. The undulations which can be seen on the first fiber section are due to variations in the backscatter factor along the fiber length [17]. There is a large spread in the apparent splice losses, including some which show an apparent gain, due to differences in backscatter factor between fiber sections. The real-time dynamic range of the OTDR is demonstrated by the visibility of the splice at 18.6 km, which is 15 dB one way down the fiber. The 4-percent Fresnel reflection from the far end of the fiber is also clearly visible in Fig. 5(e). Fig. 5(f) illustrates the gating operation of the AOD. In this instance, it is off for the first part of the backscatter trace and is switched on at 11 km.

The backscatter signal obtained from the entire length after averaging is shown in Fig. 6 plotted on a logarithmic scale. The far end has been index-matched to eliminate the Fresnel reflection. The trace was averaged in three sections with 10^6 averages used for the final part. The Rayleigh scatter signal remains above the noise floor at the far end of the fiber at 39.5 km thus confirming the 30-dB dynamic range of the OTDR which was predicted from the effective launch power and receiver sensitivity figures.

The system described does not use any components which cannot be incorporated readily into a field-portable apparatus. Nevertheless, the dynamic range with a semiconductor laser source compares favorably with previous results where a high power laser was used [6], [9], [11]. In order to demonstrate the extra dynamic range achievable when such a light source is available, the laser diode was replaced by a Nd:YAG laser. The laser is continuously pumped by an arc lamp, and is operated in a Q-switched mode at a wavelength of 1.32 μm to produce 1-μs FWHM pulses. The electronics of the OTDR system were triggered from the laser optical pulses with a germanium detector. The maximum probe-pulse power in accordance with the requirements discussed in Section II is now limited by the onset of nonlinear processes in the fiber. In this case, the nonlinear process with the lowest threshold is stimulated Raman generation [35]. The onset of Raman generation is determined by observing the spectrum of the probe pulse at the far end of the test fiber with a monochromator. In order to ensure the absence of nonlinear effects, the OTDR measurement is performed at an input power 3 dB below the level at which any Stokes signal is first detected. The peak power launched into the fiber is then ~1 W.

The enhancement of dynamic range with the Nd:YAG laser system is illustrated by measurements on the same 39.5-km fiber length. The real-time range is now in excess of 25 dB one way and is shown by Fig. 7(a)–(d), where the backscatter signal is visible to over 30 km. In Fig. 7(c) the final part of the fiber is shown with the far-end index-matched, whereas in Fig. 7(d) the same region is shown with a Fresnel reflection from the end. At the near end of the fiber the real-time signal-to-noise ratio is inferior to that obtained with the semiconductor laser, as there is additional noise from laser pulse amplitude variations, and also the greater coherence of the Nd:YAG laser results in variations in the observed backscatter signal level. Fig. 7(e) shows the signal from the first 5 km. A small fraction of the laser probe-pulse has also been directed onto the detector so that the noise on the backscatter trace, which is predominantly coherence noise, can be compared with the laser pulse amplitude variations.

The backscatter trace obtained from the entire fiber length after averaging is plotted in Fig. 8. The far end of the fiber has been index-matched, and 10^6 averages have again been used for acquiring the final section of the trace. The trace from the entire fiber length is free of noise, and the peak noise floor is at -41 dB. This dynamic range figure is nearly 10 dB one way greater than any single-mode figure reported previously, including measurements where the input power was well above the fiber nonlinear threshold.

VII. Conclusions

The requirements for a long-range single-mode optical time-domain reflectometer have been discussed, and a design which fulfills these requirements has been described. The OTDR system uses a low-noise optical receiver incorporating a p-i-n diode detector and a transimpedance amplifier, and the sensi-

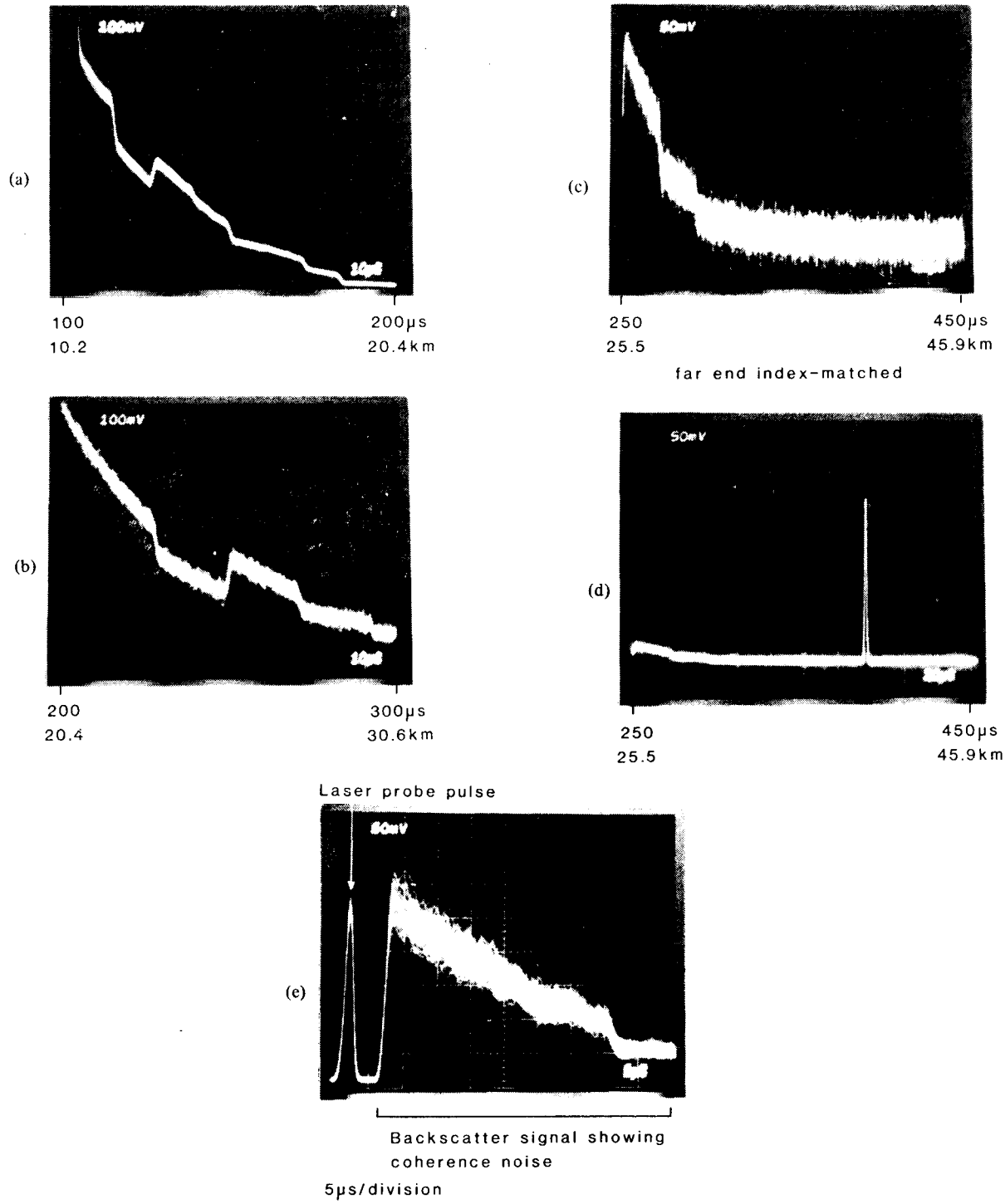

Fig. 7. Real-time backscatter traces obtained from a 39.5-km fiber with a Nd:YAG laser source.

tivity is further enhanced by multichannel digital averaging. The OTDR operates at the normal 1.3-μm single-mode fiber wavelength, although the approach can be readily extended to the 1.55-μm region. A semiconductor laser source is used to allow field portability, and a dynamic range of 30 dB one way for nonreflecting fault location with 100-m resolution has been demonstrated. Further measurements with a Nd:YAG laser source have shown an increased dynamic range of 41 dB one way, without exceeding the fiber nonlinear threshold.

ACKNOWLEDGMENT

The author is indebted to Pirelli General and to E. J. Tarbox, R. D. Birch, and S. B. Poole for providing the fiber, to A. H. Hartog for his advice and encouragement, and to W. A. Gamb-

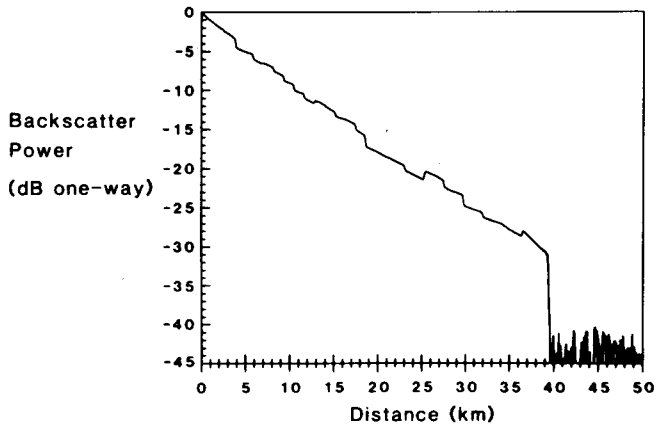

Fig. 8. Logarithmic plot of averaged backscatter trace obtained from a 39.5-km fiber with a Nd:YAG laser source.

ling and D. N. Payne for their guidance. The provision of samples of laser diodes from STL (Harlow) and detectors from Plessey Research (Caswell) and SAT (Paris) is gratefully acknowledged.

References

[1] F. P. Kapron, R. D. Maurer, and M. P. Teter, "Theory of backscattering effects in waveguides," *Appl. Opt.*, vol. 11, pp. 1352-1356, 1972.

[2] M. K. Barnoski and S. M. Jensen, "Fiber waveguides: A novel technique for investigating attenuation characteristics," *Appl. Opt.*, vol. 15, pp. 2112-2115, 1976.

[3] S. D. Personick, "Photon probe-An optical fiber time-domain reflectometer," *Bell Syst. Tech. J.*, vol. 56, pp. 355-366, 1977.

[4] K. Aoyama, K. Nakagawa, and T. Itoh, "Optical time domain reflectometry in a single-mode fiber," *IEEE J. Quantum Electron.*, vol. QE-17, pp. 862-868, 1981.

[5] P. Healey, "Multichannel photon-counting backscatter measurements on monomode fibre," *Electron. Lett.*, vol. 17, pp. 751-752, 1981.

[6] M. Nakazawa, M. Tokuda, K. Washio, and Y. Morishige, "Marked extension of diagnosis length in optical time domain reflectometry using 1.32 μm YAG laser," *Electron. Lett.*, vol. 17, pp. 783-785, 1981.

[7] S. Heckmann, E. Brinkmeyer, and J. Streckert, "Long-range backscattering experiments in single-mode fibers," *Opt. Lett.*, vol. 6, pp. 634-635, 1981.

[8] P. Healey and D. J. Malyon, "OTDR in single-mode fibre at 1.5 μm using heterodyne detection," *Electron. Lett.*, vol. 18, pp. 862-863, 1982.

[9] D. L. Philen, I. A. White, J. F. Kuhl, and S. C. Mettler, "Single-mode fiber OTDR: Experiment and theory," *IEEE J. Quantum Electron.*, vol. QE-18, pp. 1499-1508, 1982.

[10] P. Healey and D. R. Smith, "OTDR in single-mode fibre at 1.55 μm using a semiconductor laser and PINFET receiver," *Electron. Lett.*, vol. 18, pp. 959-961, 1982.

[11] K. Noguchi, "A 100-km-long single-mode optical-fiber fault location," *J. Lightwave Technol.*, vol. LT-2, pp. 1-6, 1984.

[12] M. P. Gold and A. H. Hartog, "Ultra-long-range OTDR in single-mode fibres at 1.3 μm," *Electron. Lett.*, vol. 19, pp. 463-464, 1983.

[13] S. Wright, K. Richards, S. K. Salt, and E. Wallbank, "High dynamic-range coherent reflectometer for fault location in monomode and multimode fibres," in *Proc. 9th European Conf. Opt. Commun.* (Geneva, Switzerland), 1983, pp. 177-180.

[14] A. S. Sudbo, "An optical time-domain reflectometer with low-power InGaAsP diode lasers," *J. Lightwave Technol.*, vol. LT-1, pp. 616-618, Dec. 1983.

[15] M. P. Gold and A. H. Hartog, "Improved dynamic-range single-mode OTDR at 1.3 μm," *Electron. Lett.*, vol. 20, pp. 285-287, 1984.

[16] P. Di Vita and U. Rossi, "The backscattering technique: Its field of applicability in fibre diagnostics and attenuation measurements," *Opt. & Quantum Electron.*, vol. 12, pp. 17-22, 1980.

[17] M. P. Gold and A. H. Hartog, "Determination of structural parameter variations in single-mode optical fibres by time-domain reflectometry," *Electron. Lett.*, vol. 18, pp. 489-490, 1982.

[18] M. P. Gold, A. H. Hartog, and D. N. Payne, "New approach to splice-loss monitoring using long-range OTDR," *Electron. Lett.*, vol. 20, pp. 338-340, 1984.

[19] I. L. Fabelinskii, *Molecular Scattering of Light*. New York: Plenum Press, 1968.

[20] A. J. Rogers, "Polarisation-optical time domain reflectometry: A technique for the measurement of field distributions," *Appl. Opt.*, vol. 20, pp. 1060-1074, 1981.

[21] A. H. Hartog, D. N. Payne, and A. J. Conduit, "Polarisation optical time-domain reflectometry: Experimental results and application to loss and birefringence measurements in single-mode optical fibres," in *Proc. 6th European Conf. Opt. Commun.* (York, England), 1980 (post-deadline paper).

[22] M. Nakazawa, T. Horiguchi, M. Tokuda, and N. Uchida, "Polarisation beat length measurement in a single-mode optical fibre by backward Rayleigh scattering," *Electron. Lett.*, vol. 17, pp. 513-515, 1981.

[23] J. N. Ross, "Measurement of magnetic field by polarisation optical time-domain reflectometry," *Electron. Lett.*, vol. 17, pp. 596-597, 1981.

[24] M. P. Gold and A. H. Hartog, "Measurement of backscatter factor in single-mode fibres," *Electron. Lett.*, vol. 17, pp. 965-966, 1981.

[25] E. Brinkmeyer, "Analysis of the backscattering method single-mode optical fibers," *J. Opt. Soc. Amer.*, vol. 70, pp. 1010-1012, 1980.

[26] A. H. Hartog and M. P. Gold, "On the theory of backscattering in single-mode optical fibers," *J. Lightwave Technol.*, vol. LT-2, pp. 76-82, 1984.

[27] R. D. Jeffery and J. L. Hullett, "N-point processing of optical fibre backscatter signals," *Electron. Lett.*, vol. 16, pp. 822-823, 1980.

[28] S. D. Personick, "Receiver design for digital fiber optic communication systems," *The Bell Syst. Tech. J.*, vol. 52, pp. 843-886, 1973.

[29] J. L. Hullett and T. V. Muoi, "A feedback receive amplifier for optical transmission systems," *IEEE Trans. Commun.*, vol. COM-24, pp. 1180-1185, 1976.

[30] J. E. Goell, "Input amplifiers for optical PCM receivers," *Bell Syst. Tech. J.*, vol. 53, pp. 1771-1793, 1974.

[31] A. van der Ziel, "Gate noise in field effect transistors at moderately high frequencies," *Proc. IEEE*, vol. 51, pp. 461-467, 1963.

[32] G. Pichard, J. Meslage, P. Fragnon, and F. Raymond, "HgCdTe photodiodes for long haul optical fibre communications," in *Proc. 8th European Conf. Opt. Commun.* (Cannes, France), 1982, pp. 389-393.

[33] S.E.H. Turley, G. D. Henshall, P. D. Greene, V. P. Knight, D. M. Moule, and S. A. Wheeler, "Properties of inverted rib-waveguide lasers operating at 1.3 μm wavelength," *Electron. Lett.*, vol. 17, pp. 868-870, 1981.

[34] N. Uchida and N. Niizeki, "Acoustooptic deflection materials and techniques," in *Proc. IEEE*, vol. 61, pp. 1073-1092, 1973.

[35] R. G. Smith, "Optical power handling capacity of low loss optical fibers as determined by stimulated Raman and Brillouin scattering," *Appl. Opt.*, vol. 11, pp. 2489-2494, 1972.

*

Martin P. Gold was born in London, England, in 1959. He received the B.A. degree in physics from Oxford University, England in 1980.

He joined the Optical Fibre Group in the Department of Electronics, University of Southampton, Southampton, England in 1980 as a Research Student working for the Ph.D. degree on reflectometry techniques for optical fibers. Since October 1983 he has continued his studies as a Research Fellow at the University of Southampton.